Determination of the surface structures of the GaAs(001)-(2×4) As-rich phase

Tomihiro Hashizume* and Q.-K. Xue
Institute for Materials Research (IMR), Tohoku University, Sendai 980-77, Japan

A. Ichimiya
Department of Applied Physics, Nagoya University, Nagoya, Japan

T. Sakurai
Institute for Materials Research (IMR), Tohoku University, Sendai 980-77, Japan
(Received 15 August 1994)

Field-ion scanning tunneling microscopy (STM) and *in situ* reflection high-energy electron diffraction (RHEED) have been used to study the atomic structures of the As-rich GaAs(001) surfaces grown by molecular-beam epitaxy and migration-enhanced epitaxy. The (2×4) α, β, and γ phases and the $c(4\times4)$ phase have been investigated in a systematic manner, controlling the As surface coverage. The high-resolution STM images show that the (2×4) α, β, and γ phases all have the same unit structure in the outermost surface layer, which consists of two As dimers and two As dimer vacancies. Various structure models proposed for the (2×4) phases are examined based on the STM observations and dynamical calculation of the RHEED spot intensities. We now propose the following model: The α phase is the two-As-dimer model proposed by Farrell and Palmstrom with relaxation incorporated by Northrup and Froyen. The surface coverage of the α phase is 0.5 ML of As. The β phase is the two-As-dimer model proposed by Chadi. The surface coverage of the β phase is 0.75 ML of As. The so-called γ phase is characterized by its small domains separated by open areas. The domains consist of the same local structure as the β phase and the open areas between them have a disordered As double-layer structure similar to that of the $c(4\times4)$ phase. The γ phase is, thus, no more than the mixture of the β phase and the $c(4\times4)$ phase with the surface As coverage varying between 1.75 and 0.75 ML depending on the growth conditions. Our structure model for the As-rich GaAs(001) surface is consistent with most of the observations reported.

I. INTRODUCTION

Surface reconstructions of the GaAs(001) surface grown by molecular-beam epitaxy (MBE) (Refs. 1–3) have been studied extensively because of their technological and scientific interest. This surface exhibits various symmetries of $c(4\times4)$, 2×4 [including the off-phase $c(2\times8)$], 2×6, 4×2 [including $c(8\times2)$], 4×6, and others depending on the surface coverage and the experimental conditions of the MBE. The As-rich (2×4) and $c(4\times4)$ phases are the most intensively studied, since the As-rich condition is known to be most important in the technological applications of MBE. The surface stoichiometry and structure have been investigated by various surface-sensitive techniques, such as reflection high-energy electron diffraction (RHEED),[4–15] low-energy electron diffraction/Auger-electron spectroscopy (LEED/AES),[16–20] photoemission spectroscopy (PES),[21–23] work-function measurement,[20] x-ray diffraction,[24] x-ray-photoelectron diffraction (XPD),[25] reflectance-difference spectroscopy (RDS),[26] high-resolution electron energy-loss spectroscopy (HREELS),[27] secondary-electron intensity measurement,[28] medium-energy ion scattering (MEIS),[29] and scanning tunneling microscopy (STM).[30–38] Total-energy electronic-structure calculations have also been employed lately to examine the energetics in determining the surface structures.[39–43]

Based on these experimental and theoretical studies, some general features about the structure of the GaAs(001) (2×4) As surfaces have emerged. As for the ideal bulk-terminated GaAs(001) As surface, each surface As atom has two dangling bonds and is energetically nonfavorable. Thus two adjacent As atoms form a dimer along the [$\bar{1}$10] direction and reconstruct with 2× periodicity, similar to the case of the Si(100) surface.[3] Each As dimer pair possesses two dangling bonds. The energy levels of these dangling bonds can be estimated from the s and p atomic levels following the diagram derived by Harrison.[44] Based on this diagram, the dangling-bond energy level of As lies below the valence-band maximum and should be filled, whereas the dangling-bond energy level of Ga lies above the conduction-band minimum and should be empty. Instead of assuming asymmetric As dimers for explaining the 4× periodicity along the [110] direction,[21,22] the idea of "As-dimer vacancy" was introduced theoretically by Chadi[39] and was confirmed experimentally by using STM.[30] The formation of As-dimer vacancies has been interpreted as the result of avoiding possible charge accumulation which are energetically unfavorable (the so-called electron-counting model).[7,45] The simplest structure for the 2×4 unit structure to conserve the charge neutrality can be achieved by removing one As dimer

from every four As dimers.[45]

Although it is now well established and accepted that the (2×4) symmetry is constructed from As dimers and As-dimer vacancies, there are some controversial models of the (2×4) unit structures suggesting the presence of Ga on the top layer (see Sec. III D for the discussion of Falta's model[29]). Chadi first introduced As-dimer vacancy models based on tight-binding-based total-energy calculations, and proposed two possible models: (a) three As dimers and one dimer vacancy in a unit [Fig. 1(a)], and (b) two As dimers and two dimer vacancies in a unit [Fig. 1(b)] at the outermost surface layer.[39] In the case of model (b), one of the second-layer Ga pairs is also removed. Although both models are calculated to have almost the same stability in energy, model (b), the two-As-dimer model, was later discarded by Larsen and Chadi based on the growth kinetics consideration.[9] Chadi also pointed out another possible vacancy model which retains all four pairs of the second-layer Ga atoms [Fig. 1(c)].[39] However, the total energy of this model is higher by 1.6 eV per unit than models (a) and (b), and was discarded.[39]

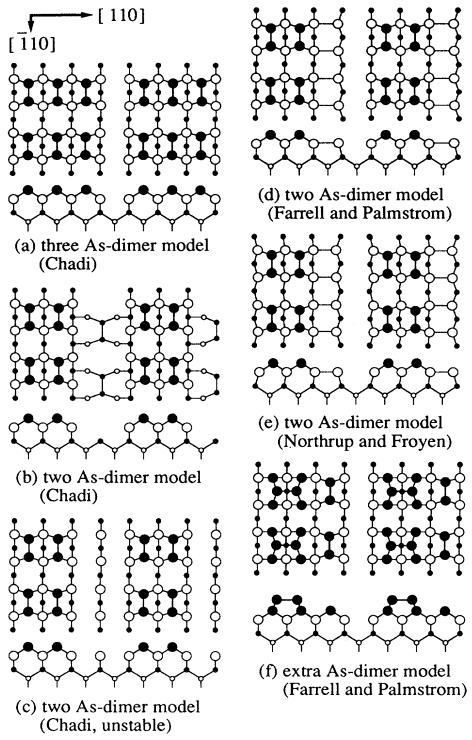

FIG. 1. Schematic representations of the GaAs(001)-(2×4) surface reconstruction models. (a) Three-As-dimer, (b) two-As-dimer, and (c) (unstable) two-As-dimer models proposed by Chadi (Ref. 39), (d) two-As-dimer model proposed by FP for the (2×4) α phase (Ref. 10), (e) model (d) modified including the second-layer Ga relaxation by NF (Ref. 42), and (f) extra-As-dimer model proposed by FP for the (2×4) γ phase (Ref. 10). Filled circles denote As atoms and open circles denote Ga atoms. Both top and side views are shown for each model. The As surface coverages are (a) 0.75, (b) 0.75, (c) 0.5, (d) 0.5, (e) 0.5, and (f) 1 ML.

Frankel *et al.* analyzed the HREELS spectra of chemisorbed atomic hydrogen on the $c(2\times8)$ phase and concluded that both Ga-H and As-H species exist on the surface, which strongly indicates the existence of As-dimer vacancy.[27] They proposed the three-As-dimer model, the same as Chadi's [Fig. 1(a)] and another vacancy model with a different As/Ga surface stoichiometry [Fig. 1(d), with second-layer Ga dimerization to Fig. 1(c) but without relaxation].[27]

Undisputable confirmation of the As vacancy model was given by the STM observation of Pashley *et al.*[30] They prepared the sample in an *ex situ* MBE system, capped the sample with As for protection prior to transferring the sample through air into the STM apparatus, and removed the As overlayers by a brief heating before the STM study.[30] The STM images clearly showed that the (2×4) periodicity is due to a regular array of As dimers and As-dimer vacancies. They also discussed an antiphase boundary along the [$\bar{1}$10] direction which produces the $c(2\times8)$ phase from the (2×4) unit. By analyzing their images of the (2×4) unit, they concluded that the STM images are best accounted for by the three-As-dimer model of Chadi [Fig. 1(a)]. Biegelsen *et al.* prepared the sample in the *in situ* MBE chamber and reported that the (2×4) phase consisted of three As dimers at the outermost surface layer,[31] supporting Pashley's observation.[30] However, they also observed the (2×4) unit consisting of two As dimers at the outermost surface layer when the surfaces were annealed longer or at higher temperatures or grown with lower As_4/Ga flux ratios.[31]

Larsen and Chadi have discussed the structure amplitude of the RHEED fractional-order spot intensities for the criterion in the selection of surface structure models.[9] The method they used was essentially a kinematical calculation. They found that models (b) and (c) give quite small values of the (0 $\frac{2}{4}$) spot intensity if only the As atoms of the outermost surface layer are taken into account.[9] Farrell and Palmstrom (FP) performed a systematic analysis of the RHEED experiment and classified the (2×4) phase into three (α, β, and γ) phases depending on the characteristics in the fractional order ($\frac{1}{4}$, $\frac{2}{4}$, and $\frac{3}{4}$) RHEED spot intensities and preparation conditions.[10] According to their analysis, the $\frac{2}{4}$ spot intensity is relatively weak compared with $\frac{1}{4}$ and $\frac{3}{4}$ intensities for the α phase, is strong and equal to $\frac{1}{4}$ and $\frac{3}{4}$ for the β phase, and is absent for the γ phase. They performed a kinematical RHEED calculation to analyze these data, and proposed that the outermost unit structure of the α, β, and γ phases is as follows (PF scheme). The α phase is composed of two As dimers [Fig. 1(d), with the second-layer Ga dimerization]. This model assigned for the α phase was later examined by Northrup and Froyen (NF),[42] and the relaxation of the second-layer Ga atoms were introduced for the stability of the model [Fig. 1(e)]. The unit structure of the β phase PF proposed is Chadi's three As dimers [Fig. 1(a)]. The γ phase is assigned to the model which has an extra As dimer sitting on the β surface along the [110] direction [Fig. 1(f)].[10] Based on the FP scheme, the As coverage is 0.5 ML for the α

phase, 0.75 ML for the β phase, and 1.0 ML for the γ phase, consistent with that expected from the preparation condition for each phase.

Many people have been using the FP scheme since then; three- or two-As-dimer models were chosen depending on the experimental conditions and results obtained. The important problem for the GaAs(001)-2×4 phases appeared to be solved.[12–15,26,41,42] However, Heller, Zhang, and Lagally, based on their *in situ* STM observations recently reported that the two-As-dimer unit at the outermost surface layer is dominant, and claimed that the three-As-dimer unit exists only under special circumstances.[33] Wassermeier *et al.* and Bressler-Hill *et al.* also claimed that the two-As-dimer unit is dominant.[34] In contrast, Gallagher, Prince, and Willis analyzed their STM images and supported the three-As-dimer unit.[35] Most recently, Falta *et al.* performed a MEIS experiment on the *ex situ* (decapped) MBE-grown GaAs(001) surfaces, and proposed a model in which the first layer of the (2×4) phase may contain both Ga and As atoms, in contrast to the commonly accepted As-terminated models.[29]

Recognizing these unsettling situations for the MBE-grown 2×4 phase, we have applied our combined MBE-STM apparatus to the systematic study of the surface structures of various GaAs(001) phases.[36–38,46] The MEE (migration-enhanced epitaxy) technique[47] was introduced in the STM investigation, which allowed us to control the surface stoichiometry in a wide range from As rich to Ga rich. We also applied the dynamical RHEED calculation to the analysis of the RHEED data we obtained simultaneously with the STM measurements in order to account for multiple scattering, concluding the fact that the kinematical RHEED calculation does not appear to reflect the real situation in the spot intensity profile.

Based on the high-resolution STM images with simultaneous RHEED observations and dynamical RHEED calculations, we now propose the unified (2×4) unit model which consists of two As dimers and two dimer vacancies at the outermost surface layer.[38] We provide detailed and quantitative analyses of the STM images of the (2×4) α, β, and γ phases, and the surface properties derived from the detailed structure models are discussed in relation to the results previously obtained by other groups.

II. EXPERIMENT

A. General

The experiments were carried out in an ultrahigh vacuum (UHV) FI-STM (field-ion scanning tunneling microscope) (Ref. 48) which was combined with a small commercial MBE system (ULVAC JAPAN, Ltd.) through a 2–3/4 in.- gate valve. There are six Knudsen cells and individual shutters are controlled by a personal computer. The two mechanical feedthroughs positioned horizontally with 90° rotated transport the sample between the MBE and STM sections smoothly and quickly without disturbing the UHV conditions. The base pressure of the STM and MBE chambers is 4×10^{-11} and 1×10^{-10} Torr, respectively.

The GaAs(001) sample was cut from on-axis wafers (dopant Si, 1×10^{18} cm^{-3}), chemically etched in a standard 4:1:1 mixture of H_2SO_4:H_2O_2:DIH_2O, and was mounted on the sample holder with indium. The sample was outgassed at 400 °C in the MBE chamber overnight. Surface oxides were removed by annealing at 600 °C in an As_4 flux.[2,4] The buffer layers were then grown at a growth temperature in the range of 540–630 °C, an As_4/Ga flux ratio of ~30, and a growth rate of 0.15 μm/h, being monitored by the RHEED intensity oscillation. The Si doping level was calibrated by SIMS (secondary-ion-mass spectrometry) and kept below 1.5×10^{18} cm^{-3} in the present work, in order to minimize surface defects induced by dopants.[32] The quenching of the sample was performed by removing the sample mounted on the small sample holder (Ta made, $3\times12\times24$ mm^3 in size) out of the MBE growth station and transferring to the STM chamber typically in 2–3 s. We estimate the quenching rate of the sample holder to be approximately 50 °C/s by IR thermometer measurements.

B. RHEED measurement

The RHEED intensity profiles were recorded both during the sample preparation (at elevated temperatures) and after the STM observation (at room temperature), and we found that the spot intensities were essentially the same for both cases, implying that the quenching rate is sufficiently high with a small heat capacitance of the sample holder. The kinetic energy of the electron beam was 10 keV, and the angle of incidence was chosen to be 1.6°±0.2° in the [$\bar{1}$10] azimuth. FP claimed that they used 0.07° (1.3 mrad) to minimize the undesired multiple scattering.[10] We question the validity of the claim of FP. The simple relationship between the angle of incidence and the RHEED spots dictates that the angle of incidence has to be larger than at least 1.2° in order to observe the $\frac{3}{4}$ or higher-order spots. When the angle of incidence becomes smaller, the overlapping of the Ewald sphere with the reciprocal-lattice rods associated with the zeroth Laue zone becomes smaller. Under this situation, we can observe the zeroth Laue zone spots only if the reciprocal-lattice rods have sufficiently broadened width (because of the imperfections of the surface) enough to cross over with the Ewald sphere. Then we cannot reliably analyze the relative intensities of the diffraction spots, since the Ewald sphere is not cutting the center of the reciprocal-lattice rods. The angle of incidence of 1.6° was chosen in the present observations for this reason. (The basic idea can be found in Ref. 49 and in many textbooks on diffraction analysis.)

C. Sample preparation of the (2×4) and c(4×4) phases

We have followed the sample preparation method described by FP (Ref. 10) and obtained $\frac{1}{4}$, $\frac{2}{4}$, and $\frac{3}{4}$ fractional-order spot intensity profiles consistent with those described by them, although the details of the

RHEED patterns could not be compared since no comprehensive data have been published about the detailed RHEED spot intensities for the α, β, and γ phases. The most stable β phase was prepared by annealing the substrate at the growth temperature, maintaining the As_4 flux until the $\frac{2}{4}$ intensity grew comparable with the $\frac{1}{4}$ and $\frac{3}{4}$ intensities. The wide range of growth temperatures (540–630 °C) could be used for the β phase.

We have used three different methods to prepare the $c(4\times4)$ and (2×4) phases.

(i) The α, γ, and $c(4\times4)$ phases were prepared by annealing the substrate which exhibits the β phase for several minutes at 640 °C, 510 °C, and below 490°C, respectively, maintaining an As_4 flux. Taking into account the high vapor pressure of As, the $c(4\times4)$ phase is known to be the most As-rich phase.

(ii) The γ, β, and α phases were also obtained from the $c(4\times4)$ phase by heating the substrate at 300, 390, and 460 °C, respectively, without the As_4 flux.[31]

(iii) The migration-enhanced epitaxy[47] technique was used as well as the regular MBE growth, mentioned above, where As_4 and Ga fluxes are alternately supplied to the substrate (by opening the As and Ga shutters alternately) to enhance the surface migration of Ga much more ($\sim$10 times) than for the case of the regular MBE.[47] We used MEE at the As_4/Ga flux ratio of 20:1 for the $c(4\times4)$ and 12:1 (2×4) γ phases, at a sample temperature of 500 °C. We have succeeded in growing the $c(4\times4)$ and (2×4) γ phases, as well as mixed phases, by this method.[37]

Because of the high vapor pressure of As, the temperatures of the sample and the As_4/Ga flux ratio critically affect the surface stoichiometry. For instance, the surface grows and both Ga and As atoms are supplied to the surface simultaneously in method (iii), while the As atoms are continuously desorbed from the surface in method (ii). In the case of method (i), the surface is under a steady-state condition with As_4 flux. In all the methods, significant amounts of mass transfer of As and Ga atoms between the surface and vacuum as well as on the surface are expected. Once the As atoms located on the surface leave the surface for migration, the Ga atoms underneath are then exposed to the vacuum and become highly mobile. Therefore, we expect sufficiently high migration of the As and Ga atoms when the $c(4\times4)$ and (2×4) phases are prepared. Therefore, the surface is nearly under steady-state conditions, and removing As atoms is essentially equivalent to adding Ga atoms.

D. STM observation

The STM images were obtained at the sample bias of $V_s=-3.5--2.0$ V with respect to the tip (grounded), and a constant tunneling current $I_t=20$ pA. The scanning area can be in the range of 20–12 000 Å in the routine measurement. We have observed that tunneling into the sample empty states ($V_s>0$) is unstable, or only gives a degraded resolution for the As-rich (2×4) phases in contrast to the GaAs(110) surface.[50] These characteristics have been noted and discussed by Pashley.[30] Keeping a low doping level enhances this effect. Dual bias imaging has been used successfully for the Be-doped p-type (2×4) phase by Wassermeier, and the effect is attributed to the difference of the Fermi-level pinning position and tip-induced band bending.[34] The contribution to the tunneling current (filled states) is attributed to the double occupied lone-pair states located on the As dimers.[34,35]

III. RESULTS AND DISCUSSION

A. STM images of the (2×4) α, β, and γ phases

Figures 2(a), 2(b), and 2(c) show typical gray scale STM images of the (2×4) α, β, and γ phases, respectively, with insets showing the enlarged small area images and the typical depth profile measured along the [110] direction. Bright features run along the $[\bar{1}10]$ direction with a spacing $d=4a_0$ [$a_0=4.0$ Å: the unit of the GaAs(001)1×1 surface] measured along the [110] direction, and is divided into units of $2a_0$ in the $[\bar{1}10]$ direction, forming (2×4) symmetry with a unit size of 8×16 Å^2.[30–35] Dark lines between them are identified as As-dimer vacancy regions as discussed by Pashley,[30] supporting the vacancy model of the (2×4) phase.[30,39]

We observe several types of defects discussed previously.[30] They are (1) complete As-dimer vacancies from the (2×4) unit which form a dark region separated by $2a_0$ along the $[\bar{1}10]$ direction; (2) a shift of (2×4) units by a_0 along the $[\bar{1}10]$ direction, which is responsible for forming the $c(2\times8)$ phases; and (3) a shift of the (2×4) units by a_0 along the [110] direction, which are called "kinks" and form an out-of-phase domain boundary in terms of the $4\times$symmetry. Defects (1) form (2×4) units separated by $d=8a_0$ measured along the [110] direction [see Fig. 2(c) for the definition of d]. Those kinks [defects (3)] may form (2×4) units separated by $d=3a_0$ and $5a_0$, if the kinks are not aligned along the [110] direction perfectly.

In the STM images, enlarged small area images and contour profiles (Fig. 2), we can clearly see that the (2×4) units at the outermost surface layer of the α, β, and γ phases all consist of two As dimers and two dimer vacancies.[38] It is interesting to note that the detailed analysis shows that the distance between these two protrusions is not exactly a_0 but approximately 15% larger. Since STM images represent the electronic density of states and not the atomic position itself, this difference suggests that the peak position of the density of states is slightly shifted from the As-dimer position in the [110] direction, which is similar to the case calculated by Ohno for the three-As-dimer model.[41] This might be part of the reason for the erroneous assignment of the STM images to the three-As-dimer model in the past. Another reason may be because some authors measure the full width of the bright-imaged As dimers in the [110] direction assuming that the width is proportional to the number of the As dimers in a unit when the resolution of the STM images is not sufficient to resolve the individual As dimers. This procedure is obviously wrong. Also, the number of the humps and the separation of them in a unit must be analyzed for proper interpretation.

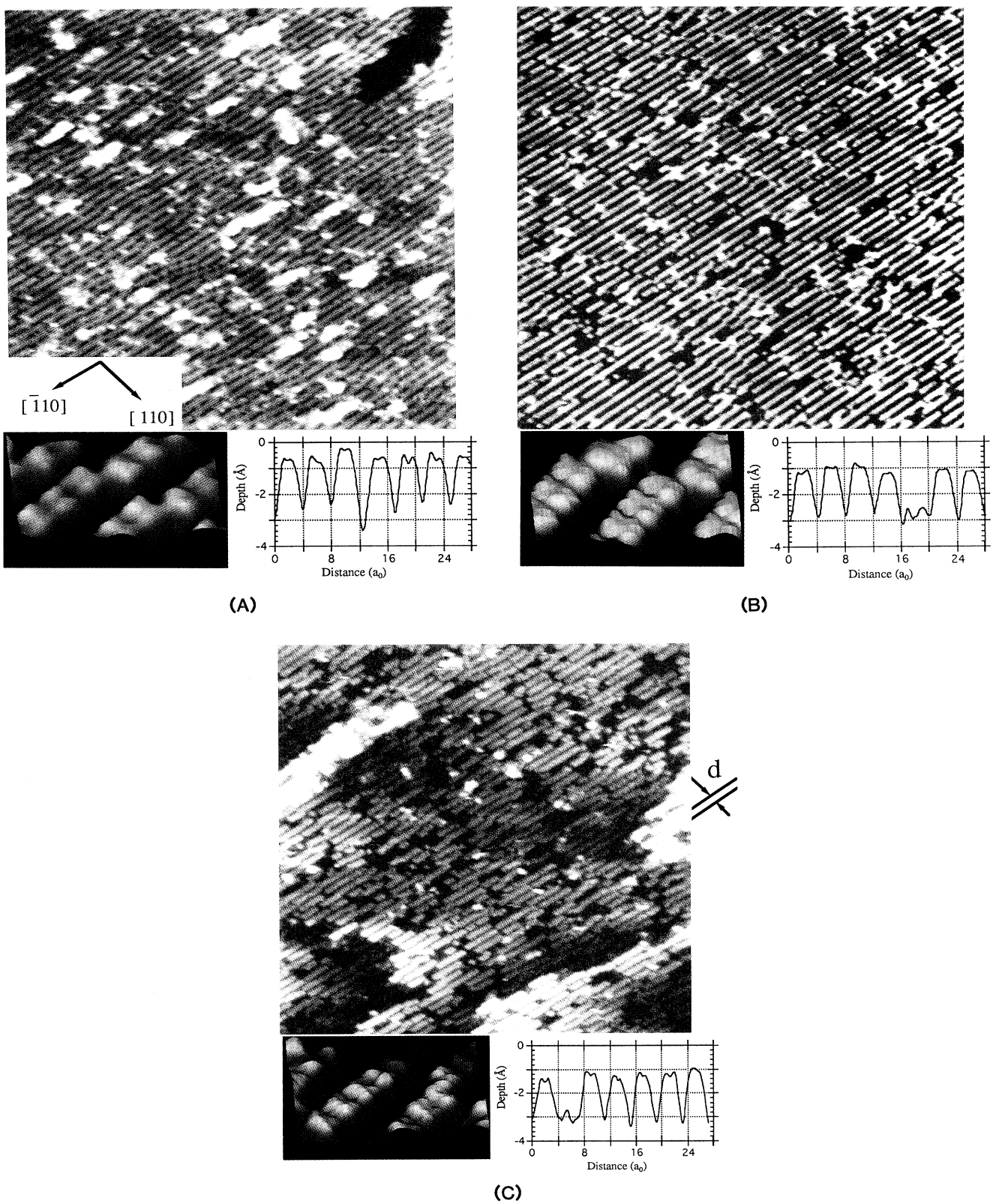

FIG. 2. Typical STM images of the (a) α, (b) β, and (c) γ phases (600×900 Å^2) together with insets showing the magnified images (three-dimensional representation) to show the details and their depth profiles measured along the [110] direction. In the STM images, it is evident that the bright lines are running along the [$\bar{1}$10] direction, separated typically by $4a_0$ along the [110] direction. All of the (2×4) unit cells of these three phases consist of two As dimers and two dimer vacancies.

We have found a simple rule for interpreting the STM images correctly, which can be applied even in the case of rather poor-resolution STM images. The rule utilizes a relationship between the number of the As dimer in the (2×4) unit at the outermost surface layer and the kink geometry. The As-dimer kink is produced with a lateral translation of the unit distance a_0 in the [110] direction. Therefore, the image of As dimers must appear continuous at the kink area, if the (2×4) or $c(2\times8)$ unit consists of three As dimers [Figs. 3(a) and 3(b)], while there should still be a space of a_0 in between these two units if the unit consists of two As dimers [Figs. 3(c) and 3(d)]. Based on this rule and a careful inspection of the kink structures, we can rule out the possibility of the three-As-dimer model for the (2×4) phases from the previously published STM images. Indeed, almost all previously published STM data claiming the three-As-dimer model fail this test, and they should be interpreted correctly in terms of the two-As-dimer model.

In the β phase [Fig. 2(b)], the dimer vacancy rows are straight and extend over 300 Å along the $[\bar{1}10]$ directions on average before any kinks. The kinks tend to align in the [110] direction, forming large domains extending up to 3000 Å along the [110] direction, demonstrating a high degree of ordering in the β phase.[36] In the α phase [Fig. 2(a)], the dimer vacancy rows are interrupted by kinks every several dimer lengths along the $[\bar{1}10]$ direction. These kinks appear to align in the [110] direction, similar to the β phase. The domain size of the α phase is typically 60 and 500 Å in the $[\bar{1}10]$ and [110] directions, respectively. In the γ phase, the kink density in the $[\bar{1}10]$ direction is similar to that of the α phase, but kinks distribute randomly and do not show any ordering in the [110] direction, unlike the case for the α phase. In the case of the γ phase, there are significant portion of open areas, where the As dimers at the outermost surface layer are missing and the structures underneath terrace are exposed. The details will be discussed in Sec. III D. The domain size of the γ phase in Fig. 2(c) is approximately 60 and 100 Å in the $[\bar{1}10]$ and [110] directions, respectively, which depends on the growth conditions.

We have examined the distribution of the separation of the neighboring (2×4) units d measured in the [110] direction. For the β phase, the nominal separation of $d=4a_0$ is dominant (98%) with small fractions of $3a_0$ ($<1\%$) and $5a_0$ ($<1\%$). For the α phase, the result is similar to the β phase with slightly higher fractions for both $3a_0$ (8%) and $5a_0$ (4%), implying a slightly higher kink density compared with the β phase. For the γ phase, the distribution of d varies greatly depending on the detailed sample preparation conditions. The distribution of d for the case of the surface shown in Fig. 2(c) is $4a_0$ (63%), $7a_0$ (15%), $3a_0$ (8%), $5a_0$ (3%), and $>7a_0$ (11%). This result shows that the γ phase is characterized by the small size of the (2×4) phases which are separated from the open area typically by $d=7a_0$.

Detailed quantitative analysis of the STM data can yield useful information about the subsurface structures. The depth profiles of the STM images measured in the [110] direction for the α, β, and γ phases show distinct differences between the α and β (γ) phases. Typically, we do not see any structure between the dimers in the α phase [the depth profile of Fig. 2(a)], while we regularly observe one or two faint line protrusions in the vacancy region of the β (γ) phases [the depth profiles of Figs. 2(b) and 2(c)]. Figure 4 summarizes the depth profile in the As-dimer vacancy measured from the position of As dimers at the outermost surface layer as a function of separation d of the neighboring (2×4) units (in unit of a_0). The measured depth for the regular (2×4) region, $d=4a_0$, is 2.1 ± 0.3 Å for all α, β, and γ phases. This measured value is smaller than the expected value of 2.8 Å$=h$, the bilayer depth of the GaAs(001) surface. We interpret this as a tip effect; that is, depth-to-width ratio of the vacancy region is too large to image the bottom. However, in the case of the separation $d>5a_0$, we ob-

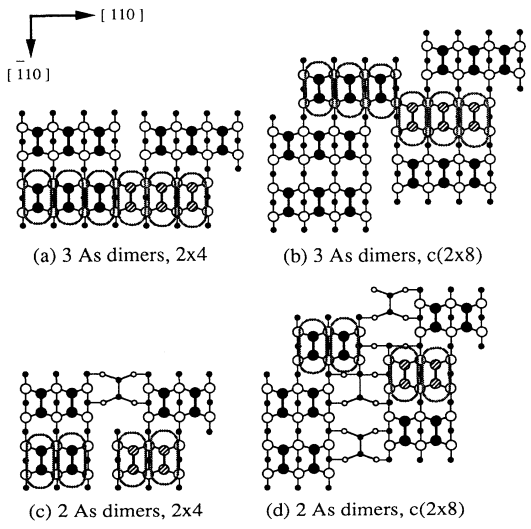

FIG. 3. Schematic STM images showing the relationship between the kinks and As-dimer arrangements nearby for the 2×4 and $c(2\times8)$ phases, based on the two-As-dimer and three-As-dimer models. If the unit consists of three As dimers, the As dimers make direct contact with the adjacent As dimers at the kink position, while there is always a gap of one-As-dimer width if the unit consists of two As dimers.

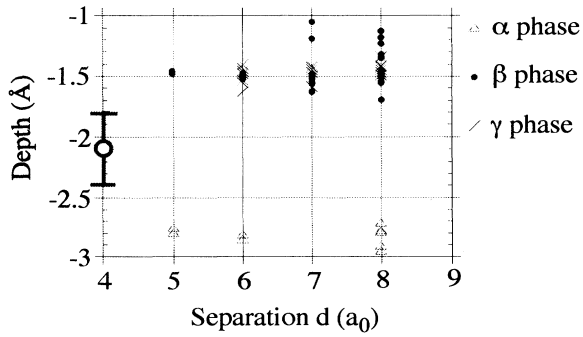

FIG. 4. Plot of the depth height of the dimer vacancy region for three different phases, measured from the position of the top-layer As dimers as a function of the separation d (in unit of a_0).

serve a reasonable depth in the α phase, which is approximately 2.8 Å$=h$, while the depth in the β (γ) phase is about 1.4 Å, one half of the bilayer depth ($1/2h$).

Since we are imaging the filled density of states, we observe the As atoms as protrusions and the dangling bonds of Ga atoms are not imaged. When we examine the models of (2×4) phases shown in Fig. 1, no structure should produce the depth height of $1/2h$ at the As vacancy regions. Thus the observation of the $1/2h$ depth for the β and γ phases in Fig. 4 implies that there must be some unknown subsurface structure in the vacancy region for the case of the β and γ phases. This observation provides us with sufficient information to discuss the subsurface structures.

B. Dynamical RHEED analysis of the (2×4) α, β, and γ phases

In order to fully understand the structures of the α, β, and γ phases, we calculated the RHEED spot intensities for the possible (2×4) models using the dynamical theory developed by Ichimiya.[51] Although it has been known that the dynamical effect is very important for the analysis of the GaAs(001) surface,[9] a systematic analysis using dynamical RHEED calculation has never been performed, most likely due to the lack of detailed knowledge of the surface structure.[38] In the present calculation, 19 beams in the zeroth Laue zone of the [$\bar{1}$10] incidence were taken into account. As the RHEED intensities in the zeroth Laue zone are insensitive to the displacement lateral to the incident direction, relaxations along the [$\bar{1}$10] direction are not taken into account.[51]

Basic structure models we used for the analysis are described in Figs. 1(a)–1(f). In general, we have assumed that the As dimers are contracted by 0.2 Å perpendicular to the surface in order to form dimers without changing the As-Ga bond length, and have no displacement along the [110] direction. Other atoms were assumed to have no relaxation from the bulk positions. We also examined the influence of the small displacement of the atom positions to the spot intensities. The rocking curves for the five zeroth-order Laue zone reflections (0 0), (0 $\frac{1}{4}$), (0 $\frac{1}{2}$), (0 $\frac{3}{4}$), and (0 1) were calculated, and the spot intensities were obtained by averaging over the incidence angle of ±0.2°.

One set of the RHEED intensity rocking curves for the case of the Chadi's two-As-dimer model are reproduced here, in order to demonstrate the full extent of our dynamical calculation (Fig. 5). The parameters used for this model in the dynamical calculation are shown in Fig. 6. These rocking curves are in good agreement with the current experiment (10 keV), as well as those obtained by Lasen *et al.*,[52] although there are some angle shifts due to the energy difference between their experiment (12.5 keV) and ours. We wish to point out that small changes of these parameters do not produce significant changes in the relative values of the spot intensities. Furthermore, it is clearly demonstrated here that the incident angle must be larger than 0.8° to observe the $\frac{2}{4}$ feature, and than 1.3° to observe the $\frac{3}{4}$ feature at all, once again disproving FP's claim about the small angle of incidence. The fully detailed account of the RHEED calculation will be published elsewhere.[53]

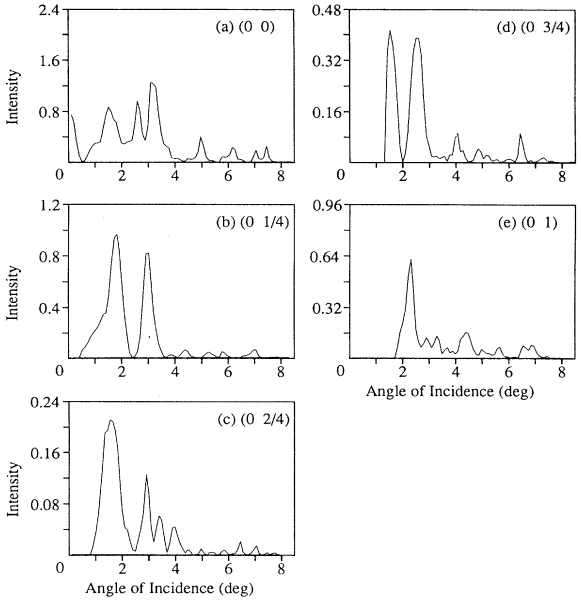

FIG. 5. The calculated rocking curves for (a) (0 0) spot, (b) (0 $\frac{1}{4}$) spot, (c) (0 $\frac{2}{4}$) spot, (d) (0 $\frac{3}{4}$) spot, and (e) (0 1) spot for Chadi's two-As-dimer model [Fig. 1(b)].

In order to compare qualitatively the theory and experiment, we used a photomultiplier with pinpoint fiber optics to measure the RHEED spot intensities. The observed RHEED patterns taken at room temperature are plotted in Figs. 7(a), 7(b), and 7(c) for the α, β, and γ phases, respectively, corresponding the STM images in Fig. 2. They were then debroadened to compare with the

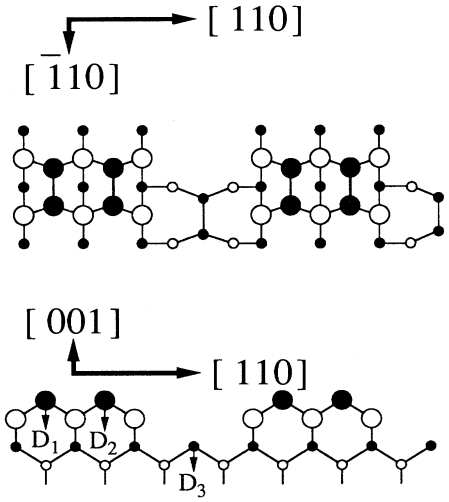

FIG. 6. Parameters used for Chadi's two-As-dimer model [Fig. 1(b)] for the dynamical RHEED calculation. Contractions of the As dimers (two on the top layer and one at the third layer) are all the same 0.2 Å.

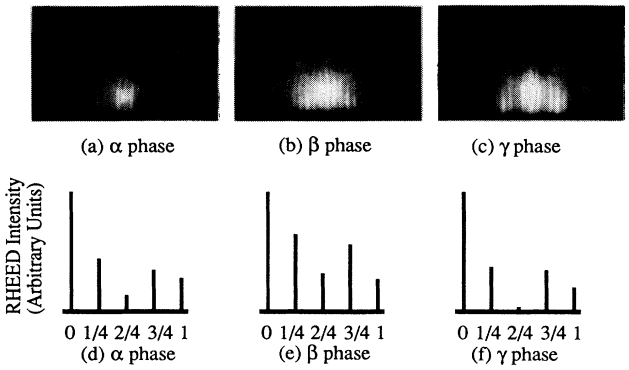

FIG. 7. Experimental RHEED patterns for the (a) α, (b) β, and (c) γ phases and their debroadened spot intensity profiles for (d) α, (e) β, and (f) γ phases. The results are in good agreement with the description by FP (Ref. 10).

theoretical results and are plotted in Figs. 7(d), 7(e), and 7(f) for the α, β, and γ phases, respectively. We confirm the characteristic features in the RHEED spot intensities as reported by FP.[10] The $\frac{2}{4}$ feature is weak for the α phase and relatively strong for the β phase with respect to the $\frac{1}{4}$ and $\frac{3}{4}$ intensities. It is almost absent for the γ phase.

The results of calculated spot intensities are summarized in Fig. 8. For the case of two-As-dimer model of Chadi [Fig. 1(b)], we calculated both without [Fig. 8(b1)] relaxation and with [Fig. 8(b2)] relaxation calculated by NF.[43] For the case of the two-As-dimer model for the α phase proposed by FP,[10] we calculated for cases of [Fig. 8(c)] without the second-layer Ga dimerization or relaxation proposed by Chadi [Fig. 1(c)],[39] [Fig. 8(d)] with the second-layer Ga dimerization but without relaxation, by FP [Fig. 1(d)],[10] and [Fig. 8(e)] after full relaxation by NF [Fig. 1(e)].[42] We also show the result of the kinematical calculation for this model taking second layer into account [Fig. 8(g)].

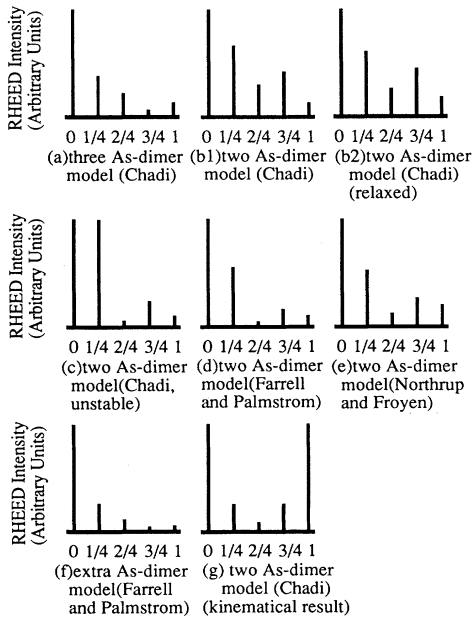

FIG. 8. Calculated RHEED spot intensity profiles for various models (a)–(f) using the dynamical theory being discussed in this text. (g) is based on the kinematical calculation.

The three-As-dimer model proposed by Chadi [Fig. 1(a)] gives a weak intensity for the $\frac{3}{4}$ fractional-order spot [Fig. 8(a)], in contrast to the result by kinematical calculation.[10] We do not find noticeable changes by varying the contraction of the As dimers from -0.4 to -0.05 Å. The inward relaxation of the second-layer Ga atoms having dangling bonds (up to 0.8 Å) yields weak intensities for $\frac{1}{4}$ and $\frac{2}{4}$ spot intensities, and does not agree with the experiment. More importantly, the three-As-dimer unit is not consistent with our STM images of the α, β, or γ phases (Fig. 2).

McCoy *et al.* analyzed the (2×4) unit structure by fitting the experimental rocking curves with the calculated ones using the dynamical RHEED theory.[14] They used Chadi's three-As-dimer unit [Fig. 1(a)] and allowed the relaxation of the first- and second-layer atoms to achieve the best fit of the rocking curves. They concluded that the center As dimer is contracted by 0.2 Å perpendicular to the surface (rumpling), and the second-layer Ga atoms have both in-plane and perpendicular relaxations.[14] They claimed that the rumpling agrees with the STM observation by Gallagher, Prince, and Willis.[35] However, the separation between two protrusions observed by Gallagher, Prince, and Willis in their high-resolution STM images can be measured to be approximately 5 Å, although they are not explicitly stating the value in their paper. The separation of the two protrusions is $2a_0=8.0$ Å expected from the rumpling claimed by McCoy *et al.*,[14] and it does not agree with the STM observation. In their dynamical analysis, McCoy *et al.* used the normalized curves to fit each fractional-order spot, neglecting the absolute value of spot intensity.[14] Although the normalized intensities and intensity peak positions of their fitted rocking curves agree well with the experimental curves, the spot intensities using their fitted atom positions are similar to the results obtained for Chadi's three-As-dimer unit without relaxation [Fig. 1(a)]. The main difference is that their coordinates yield only one quarter of intensity for the $\frac{2}{4}$ spot compared with the one for Chadi's model [Fig. 8(a)]. This is one of the confusions we discussed in Sec. I and are trying to resolve. The extra As-dimer model of (Ref. 10) [Fig. 1(f)] gives the weak $\frac{3}{4}$ spot intensity, similar to the case of the three-dimer model [Fig. 1(a)] and does not agree with any experimental results.

The two-As-dimer model proposed by Chadi [Fig. 1(b)] gives a nearly equal intensity for the $\frac{1}{4}$, $\frac{2}{4}$ and $\frac{3}{4}$ fractional-order spots [Fig. 8(b1)] and is consistent with the β phase [Fig. 7(b)]. Changing the contraction of the As dimers from -0.4 to -0.05 Å results in approximately 20% variation of the zeroth spot intensity, and the best fit to the experiment is obtained at the contraction value of approximately -0.2 Å. The kinematical calculation for this model, taking only the first layer into

account, produces the same results with two-As-dimer model discussed by FP,[10] namely zero intensity for the $\frac{2}{4}$ spot intensity. However, since they are only three out of four pairs of Ga atoms in the second layer, an interference effect is expected between the diffractions from the first and second layers, and the intensity of the reciprocal-lattice rods oscillate sinusoidally as a function of reciprocal-lattice coordinate normal to the surface (k_z).[54] If we consider the case of a less-ordered surface, the intensity of the reciprocal-lattice rod should be averaged and we obtain the spot intensities shown in Fig. 8(g). The averaged spot intensities for the (0 0, $(0\,\frac{1}{4})$, $(0\,\frac{1}{2})$, $(0\,\frac{3}{4})$ and (0 1) spots by the kinematical calculation for Chadi's two-As-dimer model are 13, 3, 1, 3, and 13, respectively [Fig. 8(g)], as the sum of the spot intensities calculated kinematically for the two-As-dimer unit (4, 2, 0, 2, and 4) and the three-As-dimer unit (9, 1, 1, 1, and 9). As a result, we observe nonzero $\frac{2}{4}$ spot intensity even for the kinematical calculation for Chadi's two-As-dimer unit. The dynamical effect further enhances the $\frac{2}{4}$ spot intensity, resulting in a good agreement with the β-phase data [Figs. 7(b) and 7(e)].

NP recently extended their first-principles calculation to Chadi's two-As-dimer model.[43] We have also calculated the spot intensities based on the detailed coordinates calculated by NP.[43] The result is shown in Fig. 8(b2). We do not observe significant differences from the original model [Fig. 8(b1)] and find that the present method is not sensitive with the exact coordinates of the individual atoms but is mainly determined by the overall arrangement of the atoms of each atomic layer. We are able to compare the calculated rocking curves with those obtained experimentally by McCoy *et al.*[14] We obtain a good agreement in the peak positions of the rocking curves as well as the absolute value of the spot intensities without significant relaxation. The full accounts of the dynamical RHEED investigations of the GaAs(001)-(2×4) phase will be published elsewhere.[53]

Various two-As-dimer models with four pairs of Ga atoms in the second layer, proposed by Chadi [Fig. 8(c)],[39] FP [Fig. 8(d)],[10] and NF [Fig. 8(e)] (Ref. 42) yield a weak-intensity 2/4 fractional-order spot in general, which is consistent with that of the α phase [Figs. 7(a) and 7(d)]. Although the $\frac{2}{4}$ spot intensity is almost absent for all the cases, the $\frac{1}{4}$ spot intensity is sensitive to the dimerization of the two Ga atoms in the second layer [Figs. 8(c) and 8(d)]. By changing the distance of Ga atoms from 4.0 [Fig. 8(c)][39] to 3.9 Å, the $\frac{1}{4}$ spot intensity changes from 1 to $\frac{1}{4}$ relative to the zeroth spot intensity. Since the spot intensities are not so sensitive to the relaxation (except for the dimerization) of the second-layer Ga atoms, the difference between the FP [Fig. 8(d)] (Ref. 10) and NF [Fig. 8(e)] (Ref. 42) units may not be discussed based simply on the spot intensity analysis, and must involve the detailed analysis of the rocking curves.[53] However, we weigh the theoretical calculations by NF and thus prefer the NF model. Another reason is that the model by NF appears to enable us to explain better the MEIS experiment of Falta *et al.*,[29] which will be discussed in Sec. III D. The present assignment for the α and β phases is also consistent with the depth profile measurement shown in Fig. 4.

In the case of the γ phase where individual domains are small and are separated typically by $d=7a_0$, the kinematical calculation can be justified, due to the diminishing dynamic effect, and the RHEED pattern should yield the diminishing $\frac{2}{4}$ fractional-order spot [Fig. 8(g)] and indeed this agrees well with spot intensities [Fig. 7(c)].

Based on these STM and RHEED results, we propose structure models for the α, β, and γ phases as follows. The α phase is the two-As-dimer model proposed by NF [Fig. 1(e)],[42] the β phase the two-As-dimer model proposed by Chadi [Fig. 1(b)][39] and the γ phase is the locally ordered β phase.

C. Transition from the $c(4\times4)$ to (2×4) γ phases

In order to analyze the detailed structure of the open area in the (2×4) γ phase, we grew the $c(4\times4)$ and (2×4) γ phases, as well as their mixed phases using migration-enhanced epitaxy (MEE).[49] This method devised by Horikoshi, Kawashima, and Yamaguchi,[49] has the following advantages: (1) surface migration of Ga is enhanced much more than the case of the regular MBE, and the surface topography is smooth enough to observe the atomic structure by STM even right after quenching the sample just after growth;[37] and (2) the surface stoichiometry can be controlled easily by changing the As and Ga shutter opening durations.[46] Figure 9 shows the surface changes as we increase the As_4/Ga flux ratio from 20:1 for the $c(4\times4)$ phase [Fig. 9(a)] to 15:1 for the mixture of the $c(4\times4)$ and γ phases [Fig. 9(d)], at a sample temperature of 500 °C. Similarly, we could obtain the (2×4) γ phase at the As_4Ga flux ratio from 12:1.

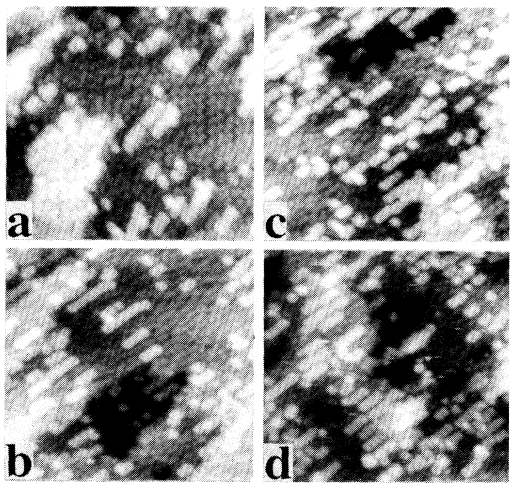

FIG. 9. A series of the STM images taken for the study of the transition from the most As-rich $c(4\times4)$ phase to the γ phase making a good use of the MEE advantage of controlling the surface stoichiometry. The As_4/Ga flux ratios are (a) 20:1, (b) 18:1, (c) 17:1, and (d) 15:1.

The STM image in Fig. 9(a) is typical for the $c(4\times4)$ phase. The unit has periodicities of $4a_0$ and $2a_0$ in the $[\bar{1}10]$ and [110] directions, respectively, forming $c(4\times4)$ symmetry. The structure model for the $c(4\times4)$ phase proposed by Biegelsen *et al.*[31] and accepted by many authors is shown in Fig. 10. This model consists of three As dimers on the As atoms in a $c(4\times4)$ unit forming the As double layer. In order to compare our data with the model, we plotted the depth profile of the $c(4\times4)$ phase along the $[\bar{1}10]$ and [110] directions in Figs. 11(a) and 11(b), respectively. Figure 11(c) shows the depth profile of the (2×4) $\gamma(\beta)$ phase for comparison. The protrusions observed by STM along the $[\bar{1}10]$ direction show two peaks (not three) separated by $2a_0$, which is consistent with the model of Biegelsen *et al.*[31] realizing the enhanced electronic density of states at the corner As dimers. The periodicity of the protrusions in the depth profile along the [110] direction is consistent with the model. Based on STM analysis, we confirm the structure model proposed by Biegelsen *et al.* for the $c(4\times4)$ phase.[31] We note that the ordering of the $c(4\times4)$ phase is not perfect,[38] and the number of As dimers can be two or even one per unit, similar to the missing dimer defects in the case of the (2×4) phases. Also, we observe As dimers which are shifted by a_0 toward the [110] direction, similar to the kink defects in the (2×4) phase. By varying the number of As dimers in a unit cell, this model can readily explain experimental results observed by x-ray diffraction.[24] We also observe the local $p(2\times2)$ area with two As dimers in a unit, which was first reported by Biegelsen *et al.*[31]

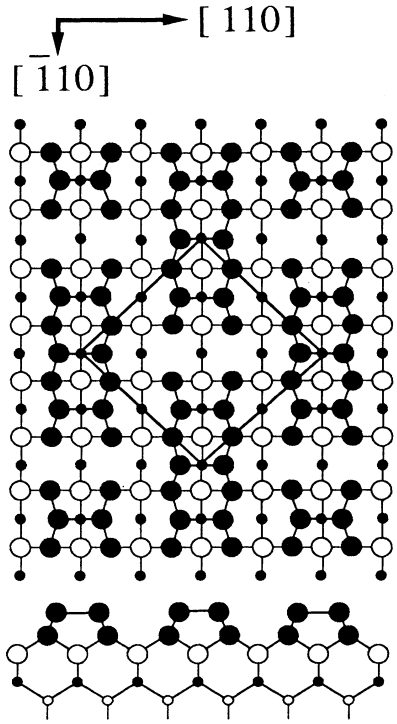

FIG. 10. Schematic of the $c(4\times4)$ phase proposed by Biegelsen *et al.*

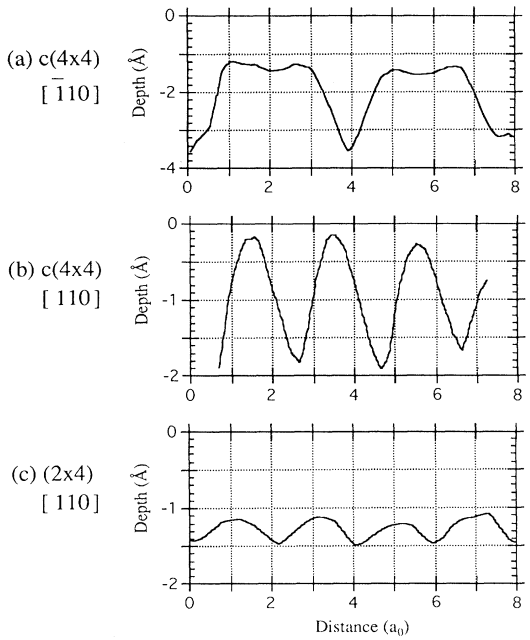

FIG. 11. Plots of height profile for (a) $c(4\times4)$ in the $[\bar{1}10]$ direction, (b) $c(4\times4)$ in the [110] direction, and (c) (2×4) in the [110] direction.

If we compare the image width of the dimers along the dimerization direction between the $c(4\times4)$ [Fig. 11(b)] and (2×4) [Fig. 11(c)] phases, we see that the As dimers in the $c(4\times4)$ phase are narrower than those in the (2×4) phase. This results in the marked difference in the STM image between the As dimers in the $c(4\times4)$ phase and those in the (2×4) phase: the former is imaged to be small round protrusions, while the latter is of the ordinary oblong shape. We believe that the difference in the chemical surroundings of As dimers in the $c(4\times4)$ phase and those in the (2×4) phase is responsible for the difference in the spatial distribution of the dangling-bond electronic states, and thus results in significantly different STM images. We also note that the As dimers in the $c(4\times4)$ phase are bonded to the As atoms and that there is no charge transfer expected from the second layer to the first layer, producing neutral As dimers on the surface. In contrast, the As dimers in the (2×4) phase are bonded to the Ga atoms, and charge transfer from the second layer is expected, resulting in the charged up As dimers. The difference in the electronic density of states has been observed and discussed by Larsen, Neave, and Joyce in their ultraviolet photoemission spectroscopy (UPS) study.[21] They observed a shallower and larger surface states peak for the (2×4) phase than for the $c(4\times4)$ phase, which appears to be consistent with the STM image size difference between the As dimers in the $\gamma(\beta)$ and $c(4\times4)$ phases. Unfortunately, there has been no theoretical calculation showing the mapping of density of states from which we can discuss the details of the STM image difference.

After understanding the difference of the STM image between As dimers in the $c(4\times4)$ unit and those in the

(2×4) unit, it is straightforward to understand the process of the $c(4\times4)$ phase transferring to the (2×4) γ phase under lesser As conditions. Even in the $c(4\times4)$ phase transferring to the (2×4) γ phase under lesser As conditions. Even in the $c(4\times4)$ phase, there are islands nucleated with the 2×4 unit structure [Fig. 9(a)]. When a slightly less As-rich condition is used, we observe more areas with the (2×4) unit compared with Fig. 9(a) [Figs. 9(b)–9(d)]. A series of MEE experiments with different As_4/Ga flux ratios shows that the (2×4) area becomes dominant with decreasing As_4/Ga flux ratio, and finally the surface becomes identical to the γ phase grown by MBE [Fig. 2(c)] at the As_4/Ga flux ratio of 12:1. In between the nucleated islands of the (2×4) phase, we still see the remaining $c(4\times4)$ phase (Fig. 9). These observations naturally lead to the conclusion that the (2×4) γ phase is formed by replacing $c(4\times4)$ units with (2×4) units under lower As conditions. Actually, if we examine the open areas in the γ phase, we frequently observe subsurface structures, and the depth of those are measured to be approximately 1.4 Å ($=1/2h$), which is shown in Fig. 2(b) and also shown systematically in Fig. 4. Thus we conclude that in the open area of the γ phase are the remaining As dimers on the third-layer As atoms, similar to the As double layer of the $c(4\times4)$ phase.

We have studied possible structures of the open area of the γ phase for the separation $d=5a_0$, $7a_0$, and $8a_0$. Figure 12 presents the structure models for those we identified based on the STM data. The abundance of the individual structures varies depending on the preparation conditions. We find that the structure (a) is most abundant (> 90%) for the case of $d=7_0$, for example.

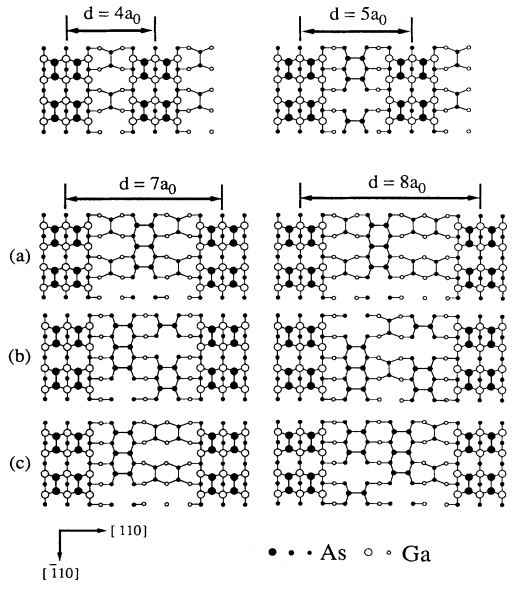

FIG. 12. Schematic representation of possible atomic structures of the open areas observed for the γ phase. The faint line structures being observed in the darkly imaged open areas show the As double layer: the building block of the $c(4\times4)$ phase.

D. Structure model for the (2×4) α, β, and γ phases

Based on the STM observations and dynamical calculation of the RHEED spot intensities, we propose the following unified model for the (2×4) α, β, and γ phases (Fig. 13): The α phase is the two-As-dimer model proposed by FP,[10] with relaxation incorporated by NF.[42] The β phase is the two-As-dimer model proposed by Chadi.[39] The γ phase is merely a mixture of the β phase and the $c(4\times4)$ phase.

In all the methods we used for preparing the surface (Sec. II), we expect significant amounts of mass transfer of As atoms between the surface and vacuum as well as on the surface. Therefore, the surface is nearly under steady-state conditions, and removing As atoms is essentially equivalent to adding Ga atoms. For the case of the γ phase, the open area with the local double layer of As has an As coverage up to 1.75 ML, the same as that of $c(4\times4)$ and the (2×4) region has an As coverage of 0.75 ML (one As dimer per unit in the third layer). Thus the γ phase, the mixture phase of the $c(4\times4)$ and (2×4) γ phases, can exhibit the As surface coverage between 1.75 and 0.75 ML. Once the sample preparation condition is chosen, the surface stoichiometry and the domain ratio of the $c(4\times4)$ and (2×4) γ phases are determined. The surface coverage of As for the (2×4) α, β, and γ, and $c(4\times4)$ phases are typically 0.5, 0.75, 1, and 1.75 ML, respectively. This agrees very well with previous results.

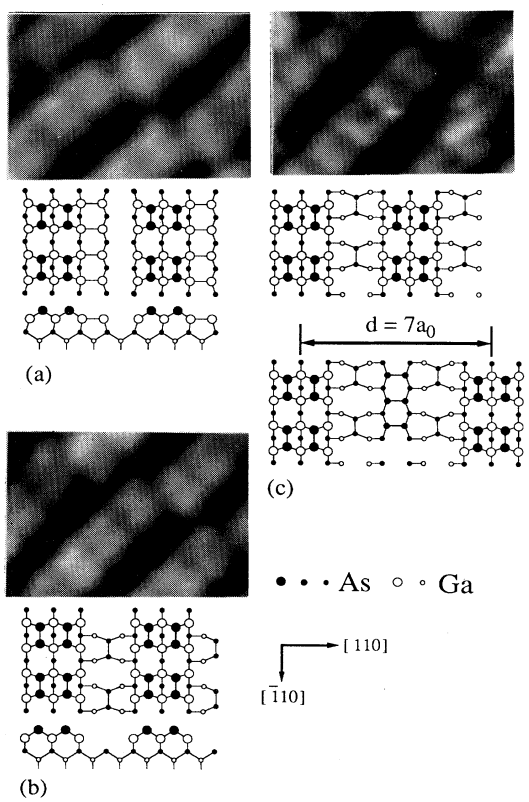

FIG. 13. Typical STM images and proposed structure models for the (a) α, (b) β, and (c) typical γ phases.

The unified model proposed here for the $c(4\times4)$ and (2×4) α, β, and γ phases may explain the most recent MEIS results by Falta *et al.*[29] by considering the fact that the Ga atoms exposed to the ion beam increase in the order from the $c(4\times4)$ to γ, β, and α phases, successively. The disagreement Falta *et al.* pointed out, regarding with the As top-layer models, concerns the absolute value in the As/Ga intensity ratio for the (2×4) α phase.[29] However, in NF's two-As-dimer model for the α phase, all first-layer As dimers, and the second-layer Ga and third-layer As atoms are shifted from the original positions; therefore, this should reduce the blocking of the scattering intensity from the sixth-layer Ga atoms which increases the Ga intensity, especially slightly off of the blocking angle, and resolve the intriguing discrepancy.

IV. CONCLUSIONS

In conclusion, we have performed simultaneous STM and RHEED studies of the MBE- and MEE-grown As-rich GaAs(001)-$c(4\times4)$ and -(2×4) α, β, and γ phases, and proposed a model. The unit cell of the α, β, and γ phases all consist of the two As dimers and two dimer vacancies, and the α and β phases have different second- and third-layer structures. The α and β phases can be accounted for best by Chadi's two-As-dimer model and Northrup and Froyen's two-As-dimer model, respectively. The γ phase is the locally ordered β phase with fractions of the $c(4\times4)$ phase.

ACKNOWLEDGMENTS

We acknowledge Dr. J. E. Northrup and Dr. S. Froyen for providing us with detailed information about the recent calculations before publication.[42,43] We also thank Professor J. M. Zhou (Institute of Physics, Academia Sinica, Beijing), Kevin Yeh (MIT), and S. Amano (ULVAC) for their valuable contributions.

*Present address: Advanced Research Laboratory, Hitachi Ltd., Saitama 350-03, Japan.

[1]A. Y. Cho, J. Appl. Phys. **42**, 2074 (1971); J. R. Arthur, Surf. Sci. **43**, 449 (1974).
[2]A. Y. Cho and J. R. Arthur, Prog. Solid State Chem. **10**, 157 (1975).
[3]A. Y. Cho, J. Appl. Phys. **47**, 2841 (1976).
[4]J. H. Neave and B. A. Joyce, J. Cryst. Growth **44**, 387 (1978).
[5]P. K. Larsen, J. H. Neave, J. F. van der Veen, P. J. Dobson, and B. A. Joyce, Phys. Rev. B **27**, 4966 (1983).
[6]B. A. Joyce, J. H. Neave, P. J. Dobson, and P. K. Larsen, Phys. Rev. B **29**, 814 (1984).
[7]H. H. Farrell, J. P. Harbison, and L. D. Peterson, J. Vac. Sci. Technol. B **5**, 1482 (1987).
[8]M. G. Knibb and P. A. Maksym, Surf. Sci. **195**, 475 (1988).
[9]P. K. Larsen and D. J. Chadi, Phys. Rev. B **37**, 8282 (1988).
[10]H. H. Farrell and C. J. Palmstrom, J. Vac. Sci. Technol. B **8**, 903 (1990).
[11]L. Däweritz and R. Hey, Surf. Sci. **236**, 15 (1990).
[12]H. Yamaguchi and Y. Horikoshi, Phys. Rev. B **44**, 5897 (1991).
[13]C. Deparis and J. Massies, J. Cryst. Growth **108**, 157 (1991).
[14]J. M. McCoy, U. Korte, P. A. Maksysm, and G. Meyer-Ehmsen, Phys. Rev. B **48**, 4721 (1993); Surf. Sci. **261**, 48 (1992).
[15]H. Nörenberg and N. Koguchi, Surf. Sci. **296**, 199 (1993).
[16]A. J. van Bommel, J. E. Chrombeen, and T. G. Van Dirschot, Surf. Sci. **72**, 95 (1978).
[17]P. Drathen, W. Ranke, and K. Jacobi, Surf. Sci. **77**, L162 (1978); W. Ranke and K. Jacobi, Prog. Surf. Sci. **10**, 1 (1981).
[18]S. P. Svensson, P. O. Nilsson, and T. G. Anderson, Phys. Rev. B **31**, 5272 (1985).
[19]J. Massies, P. Etienne, F. Dezaly, and N. T. Linh, Surf. Sci. **99**, 121 (1980).
[20]R. Duszak, C. J. Palmstrom, L. T. Florez, Y.-N. Yang, and J. H. Weaver, J. Vac. Sci. Technol. B **10**, 1891 (1992).
[21]P. K. Larsen, J. H. Neave, and B. A. Joyce, J. Phys. C **14**, 167 (1981).
[22]P. K. Larsen, J. F. van der Veen, A. Mazur, J. Pollmann, J. H. Neave, and B. A. Joyce, Phys. Rev. B **26**, 3222 (1982).
[23]T.-C. Chiang, R. Ludeke, M. Aono, G. Landgren, F. J. Himpsel, and D. E. Eastman, Phys. Rev. B **27**, 4770 (1983).
[24]M. Sauvage-Simkin, R. Pinchaux, J. Massies, P. Calverie, N. Jedrecy, J. Bonnet, and I. K. Robinson, Phys. Rev. Lett. **62**, 563 (1989).
[25]S. A. Chambers, Surf. Sci. **261**, 48 (1992).
[26]I. Kamiya, D. A. Aspnes, H. Tanaka, L. T. Florez, J. P. Harbison, and R. Bhat, Phys. Rev. Lett. **68**, 627 (1992); I. Kamiya, D. E. Aspnes, L. T. Florez, and J. P. Harbison, Phys. Rev. B **46**, 15 894 (1992).
[27]D. J. Frankel, C. Yu, J. P. Harbison, and H. H. Farrell, J. Vac. Sci. Technol. B **5**, 1113 (1987).
[28]K. Kanisawa, J. Osaka, S. Hirono, and N. Inoue, J. Cryst. Growth **115**, 348 (1991).
[29]J. Falta, R. M. Tromp, M. Copel, G. D. Pettit, and P. D. Kirchner, Phys. Rev. Lett. **69**, 3068 (1992); Comments and Reply, Phys. Rev. Lett. **70**, 3171 (1993).
[30]M. D. Pashley, K. W. Haberern, W. Friday, J. M. Woodall, and P. D. Kirchner, Phys. Rev. Lett. **60**, 2176 (1988).
[31]D. K. Biegelsen, R. D. Bringans, J. E. Northrup, and L.-E. Swartz, Phys. Rev. B **41**, 5701 (1990); D. K. Biegelsen, R. D. Bringans, and L. E. Swartz, Proc. SPIE **1186**, 136 (1990).
[32]M. D. Pashley and K. W. Haberern, Phys. Rev. Lett. **67**, 2697 (1991); M. D. Pashley, K. W. Haberern, R. M. Feenstra, and P. D. Kirchner, Phys. Rev. B **48**, 4612 (1993).
[33]E. J. Heller, Z. Y. Zhang, and M. G. Lagally, Phys. Rev. Lett. **71**, 743 (1993); E. J. Heller and M. G. Lagally, Appl. Phys. Lett. **60**, 2675 (1992).
[34]M. Wassermeier, V. Bressler-Hill, R. Maboudian, K. Pond, X. S. Wang, W. H. Weinberg, and P. M. Petroff, Surf. Sci. Lett. **278**, L147 (1992); V. Bressler-Hill, M. Wassermeier, K. Pond, R. Maboudian, G. A. D. Briggs, P. M. Petroff, and W. H. Weinberg, J. Vac. Sci. Technol. B **10**, 1881 (1992).
[35]M. C. Gallagher, R. H. Prince, and R. F. Willis, Surf. Sci. **275**, 31 (1992).
[36]J. M. Zhou, Q.-K. Xue, H. Chaya, T. Hashizume, and T.

Sakurai, Appl. Phys. Lett. **64**, 583 (1994).
[37]Q.-K. Xue, J. M. Zhou, T. Hashizume, and T. Sakurai, J. Appl. Phys. **75**, 5201 (1994).
[38]T. Hashizume, Q. K. Xue, J. M. Zhou, A. Ichimiya, and T. Sakurai, Phys. Rev. Lett. **73**, 2208 (1994).
[39]D. J. Chadi, J. Vac. Sci. Technol. A **5**, 834 (1987).
[40]G.-X. Qian, R. M. Martin, and D. J. Chadi, Phys. Rev. B **38**, 7649 (1988).
[41]T. Ohno, Phys. Rev. Lett. **70**, 631 (1993).
[42]J. E. Northrup and S. Froyen, Phys. Rev. Lett. **71**, 2276 (1993).
[43]J. E. Northrup and S. Froyen, Phys. Rev. B **50**, 2015 (1994).
[44]W. A. Harrison, J. Vac. Sci. Technol. **16**, 1492 (1979).
[45]M. D. Pashley, Phys. Rev. B **40**, 10 481 (1989).
[46]Q. K. Xue, T. Hashizume, T. Sakata, and T. Sakurai (unpublished).
[47]Y. Horikoshi, M. Kawashima, and H. Yamaguchi, Jpn. J. Appl. Phys. **25**, L868 (1986).
[48]T. Sakurai, T. Hashizume, I. Kamiya, Y. Hasegawa, N. Sano, H. W. Pickering, and A. Sakai, Prog. Surf. Sci. **33**, 3 (1990).
[49]A. Ichimiya, K. Kambe, and G. Lehmpfuhl, J. Phys. Soc. Jpn. **49**, 684 (1980); Y. Horio and A. Ichimiya, Surf. Sci. **219**, 128 (1989).
[50]R. M. Feenstra, J. A. Stroscio, and J. Tersoff, Phys. Rev. Lett. **25**, 1192 (1987).
[51]A. Ichimiya, Jpn. J. Appl. Phys. **22**, 176 (1983); **24**, 1365 (1985); Surf. Sci. **235**, 75 (1990).
[52]P. K. Lasen, P. J. Dobson, J. H. Neave, B. A. Joice, B. Bölger, and J. Zhang, Surf. Sci. **169**, 176 (1986).
[53]A. Ichimiya *et al.* (unpublished).
[54]G. M. Lagally, in *Methods of Experimental Physics* (Academic, New York, 1985), p. 237; M. Henzler, Surf. Sci. **11/12**, 450 (1982).

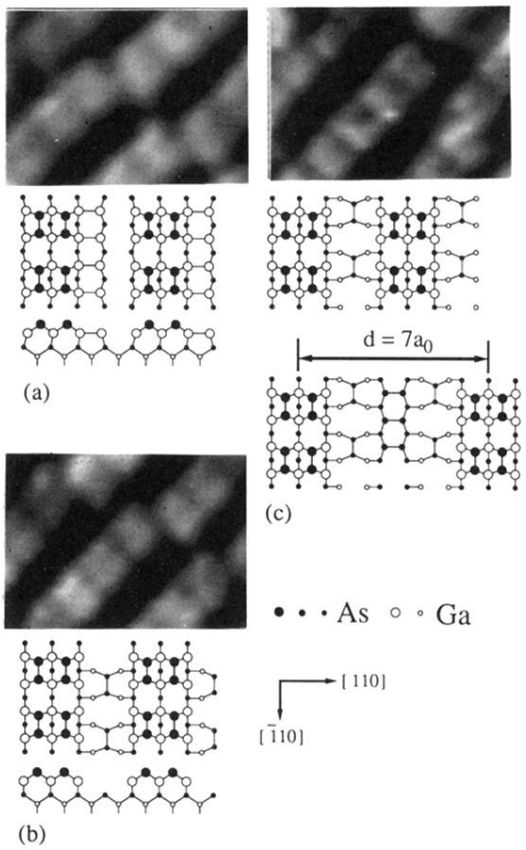

FIG. 13. Typical STM images and proposed structure models for the (a) α, (b) β, and (c) typical γ phases.

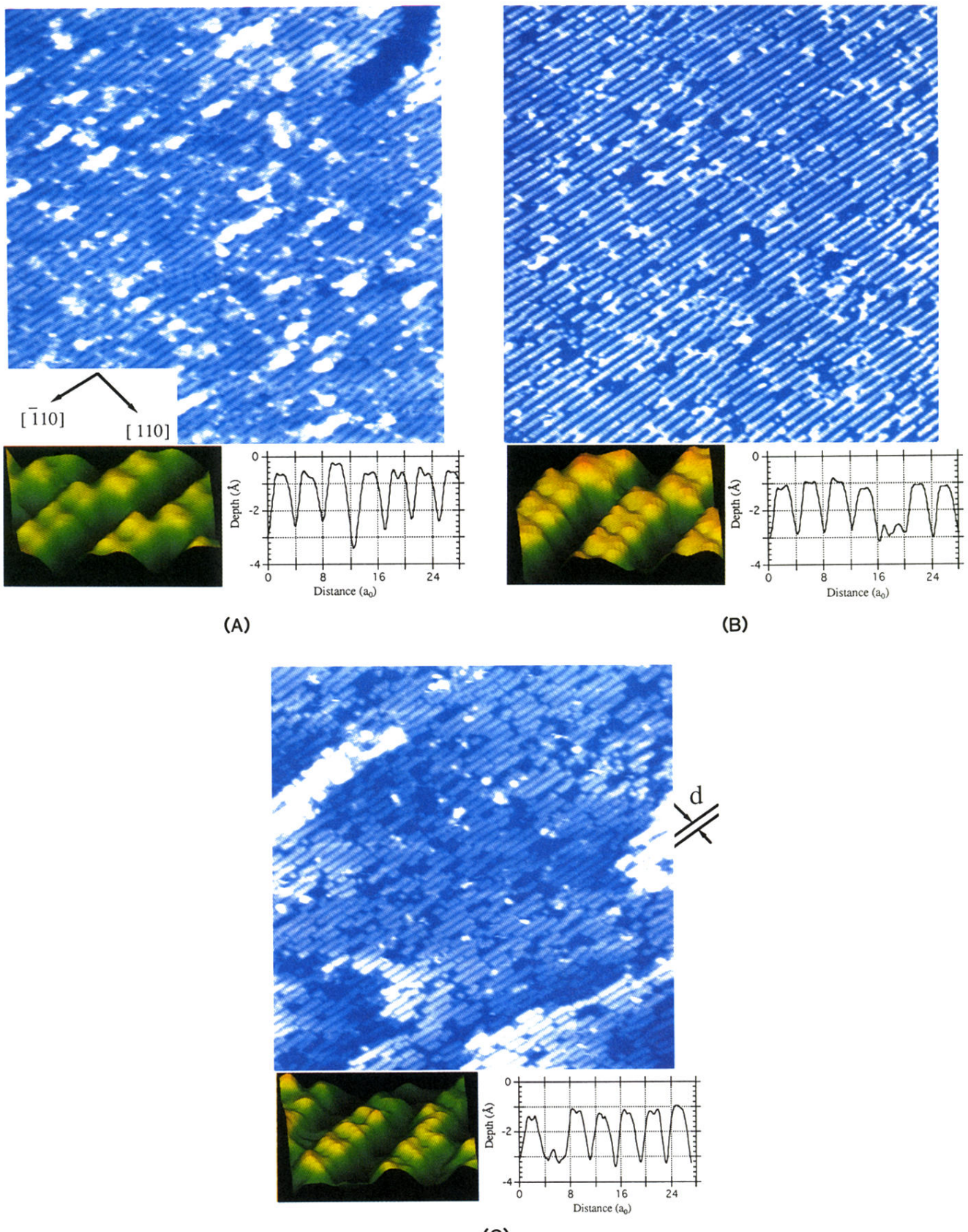

FIG. 2. Typical STM images of the (a) α, (b) β, and (c) γ phases (600×900 Å^2) together with insets showing the magnified images (three-dimensional representation) to show the details and their depth profiles measured along the [110] direction. In the STM images, it is evident that the bright lines are running along the [$\bar{1}$10] direction, separated typically by $4a_0$ along the [110] direction. All of the (2×4) unit cells of these three phases consist of two As dimers and two dimer vacancies.

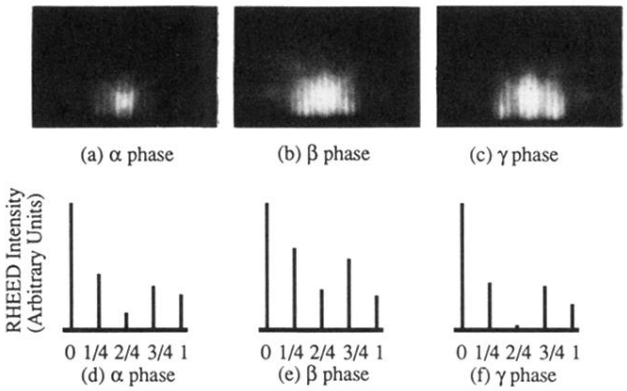

FIG. 7. Experimental RHEED patterns for the (a) α, (b) β, and (c) γ phases and their debroadened spot intensity profiles for (d) α, (e) β, and (f) γ phases. The results are in good agreement with the description by FP (Ref. 10).

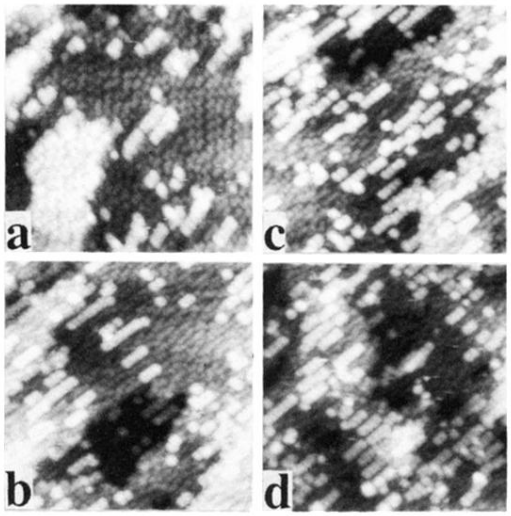

FIG. 9. A series of the STM images taken for the study of the transition from the most As-rich $c(4\times4)$ phase to the γ phase making a good use of the MEE advantage of controlling the surface stoichiometry. The As_4/Ga flux ratios are (a) 20:1, (b) 18:1, (c) 17:1, and (d) 15:1.